ChemPubSoc Europe

DOI: 10.1002/cctc.201702055

CHEMCATCHEM Communications

Photoelectrocatalytic Synthesis of Hydrogen Peroxide by Molecular Copper-Porphyrin Supported on Titanium Dioxide Nanotubes

Dogukan H. Apaydin,*[a] Hathaichanok Seelajaroen,[a] Orathip Pengsakul,[b] Patchanita Thamyongkit,[c, d] Niyazi Serdar Sariciftci,[a] Julia Kunze-Liebhäuser,[e] and Engelbert Portenkirchner*[e]

We report on a self-assembled system comprising a molecular copper-porphyrin photoelectrocatalyst, 5-(4-carboxy-phenyl)-10,15,20-triphenylporphyrinatocopper(II) (CuTPP-COOH), covalently bound to self-organized, anodic titania nanotube arrays (TiO_2 NTs) for photoelectrochemical reduction of oxygen. Visible light irradiation of the porphyrin-covered TiO_2 NTs under cathodic polarization up to −0.3 V vs. Normal hydrogen electrode (NHE) photocatalytically produces H_2O_2 in pH neutral electrolyte, at room temperature and without need of sacrificial electron donors. The formation of H_2O_2 upon irradiation is proven and quantified by direct colorimetric detection using 4-nitrophenyl boronic acid (*p*-NPBA) as a reactant. This simple approach for the attachment of a small molecular catalyst to TiO_2 NTs may ultimately allow for the preparation of a low-cost H_2O_2 evolving cathode for efficient photoelectrochemical energy storage under ambient conditions.

Two-electron oxygen reduction reaction (ORR) of dissolved oxygen (O_2) in water leads to formation of hydrogen peroxide (H_2O_2) which is a versatile, high energy product,[1] capable of participating in numerous further redox reactions and is an active species in a plethora of biological processes.[2] Solar-driven H_2O_2 formation has been proposed for chemical energy storage.[1,3–5] However, the widely used anthraquinone process for the formation of H_2O_2 is known to be energy intensive.[6] For many decades, researchers have tried to address this issue and tackle the problem by introducing metal catalysts,[7–12] core–shell structures, metal oxides, metal chalcogenides etc.[13–15] Additionally, photocatalytic reduction of O_2 to H_2O_2 by inorganic semiconductors (e.g. are ZnO, CdS and TiO_2) and organometallic complexes has been reported.[14,16–18] Recently, metal-free carbon-based catalysts has been the focus for (photo)electrochemical reduction of dissolved O_2. This class mainly includes graphitic carbon nitrides (g-C_3N_4) and organic pigments.[19–21] However, almost all of these reactions require either acidic or basic conditions which make daily applications challenging. Although there are a few examples,[22] the search for a catalyst which works under mild pH conditions is still in progress.

Here, we present a photoelectrode consisting of a porphyrin derivative, namely CuTPP-COOH (Figure 1 a), coated on TiO_2 nanotubes (NT) (TiO_2 NTs/CuTPP-COOH) for the reduction of O_2 to H_2O_2. The introduction of a carboxyl group enables the attachment of the photoactive porphyrin onto the nanostructured TiO_2 NTs.[23] CuTPP-COOH was chosen owing to ease of its synthesis as well as the appropriate energy levels to reduce O_2. We have also utilized ZnTPP-COOH for the same reaction; however the stability of this material was inferior. The high surface area of TiO_2 NTs[24] increases the number of potential catalytically active sites . In addition, the amorphous structure of TiO_2 NTs helps to anchor the CuTPP-COOH through the −COOH functional group. The reaction takes place at neutral pH and ambient temperature (22 °C). By applying moderate negative potentials between 0.0 V and −0.3 V vs. NHE (normal hydrogen electrode) and upon photoexcitation of CuTPP-COOH at $\lambda > 395$ nm, an exciton (electron-hole pair) is initially formed, as illustrated in Figure 1 b. Subsequently, the newly created hole residing in the valence band of CuTPP-COOH is recombined with an electron supplied from the external circuit, while

[a] D. H. Apaydin, H. Seelajaroen, Prof. Dr. N. S. Sariciftci
Linz Institute for Organic Solar Cells (LIOS), Institute of Physical Chemistry
Johannes Kepler University Linz
4040 Linz (Austria)
E-mail: Dogukan.Apaydin@jku.at

[b] O. Pengsakul
Petrochemistry and Polymer Science Program, Faculty of Science
Chulalongkorn University
Bangkok, 10330 (Thailand)

[c] Assoc. Prof. Dr. P. Thamyongkit
Department of Chemistry, Faculty of Science
Chulalongkorn University
Bangkok, 10330 (Thailand)

[d] Assoc. Prof. Dr. P. Thamyongkit
Research group on Materials for Clean Energy Production STAR,
Department of Chemistry, Faculty of Science
Chulalongkorn University
Bangkok 10330 (Thailand)

[e] Prof. Dr. J. Kunze-Liebhäuser, Dr. E. Portenkirchner
Institute of Physical Chemistry
University of Innsbruck
6020 Innsbruck (Austria)
E-mail: Engelbert.Portenkirchner@uibk.ac.at

Supporting information and the ORCID identification number(s) for the author(s) of this article can be found under https://doi.org/10.1002/cctc.201702055.

This manuscript is part of a Special Issue on "Supported Molecular Catalysts".

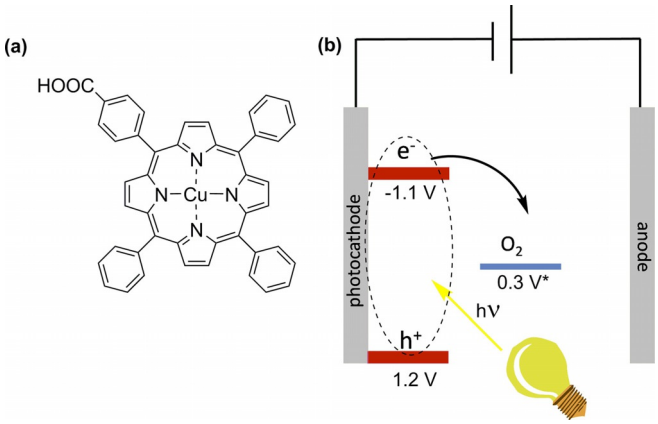

Figure 1. (a) Chemical structure of CuTPP-COOH, and (b) schematic representation of photoelectrochemical reduction of O_2. Formal potential of O_2 reduction to H_2O_2 is recalculated for pH7 from the reported literature values.[25]

the electron in the conduction band is capable of reducing the dissolved O_2 in water to H_2O_2.

Characterization of the TiO_2 NTs/CuTPP-COOH films using scanning electron micrographs (SEM, Figure S2, Supporting Information), optical imaging (Figure S3, Supporting Information) and Fourier-transform infrared spectroscopy (FTIR, Figure S4, Supporting Information) techniques is presented in the Supporting Information.

The electrochemical behavior of the TiO_2 NTs/CuTPP-COOH photoelectrodes under applied potential in Ar- and O_2-saturated conditions can be seen in Figure 2. In the absence of O_2, the illumination led to no observable increase in current with a current density (j) of approximately 1.3 $\mu A\,cm^{-2}$ at −0.3 V vs. NHE. However, under O_2 saturation and upon light illumination, the current value increased around 4 fold and reached approximately 13 $\mu A\,cm^{-2}$ at −0.3 V, signaling the reduction of dissolved O_2.

After chronoamperometry experiments, a series of constant potential electrolysis experiments were conducted to quantify the formation of H_2O_2. One of the reasonable ways for direct detection of H_2O_2, is an indirect spectrophotometric method for the quantification of the product, relying on a stoichiometric reaction of arylboronic acids with newly generated H_2O_2 under mild basic conditions to yield the respective photoactive phenolates.[26,27] In this work, *p*-nitrophenylboronic acid (*p*-NPBA) was used at pH 9, which was converted upon reaction with H_2O_2 into *p*-nitrophenol (*p*-NP), for which absorption could be observed by using UV/Vis spectrophotometry at 405 nm. A calibration curve for quantitative determination of H_2O_2 in a concentration range between 0.5 μM and 20 μM is shown in Figure 3. The detailed procedure for the preparation of the standard solutions can be found in the Supporting Information.

After each constant potential electrolysis measurement, an aliquot of 100 μL was pipetted from the electrolyte solution and then transferred into a vial containing the *p*-NPBA and carbonate buffer. Amounts of H_2O_2, reflected by those of newly formed *p*-NP, between 1.9 μM and 3.9 μM were observed

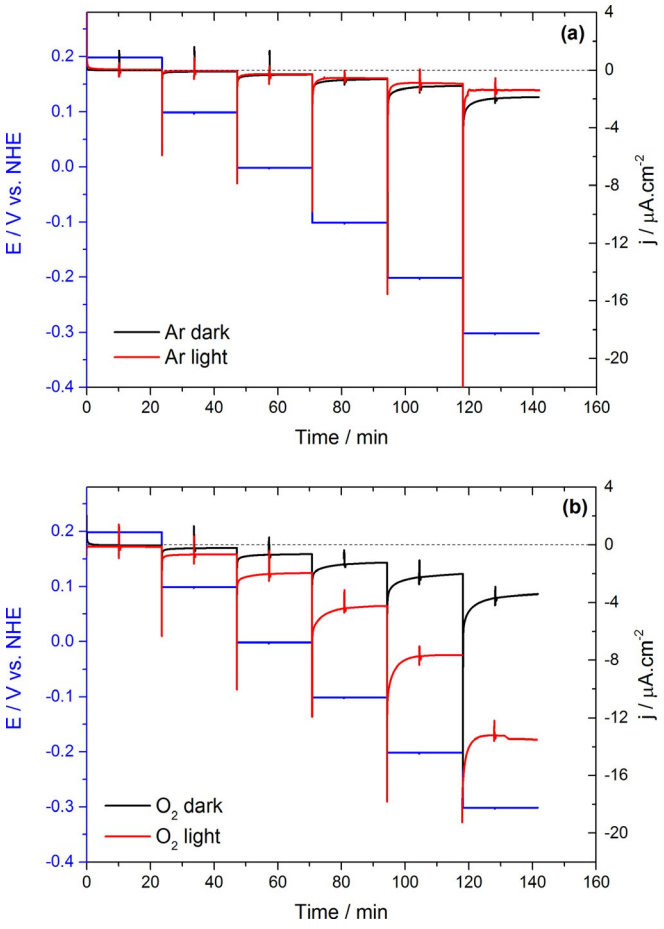

Figure 2. Chronoamperometry of CuTPP-COOH-coated electrodes in the dark (black solid line) and upon illumination (red solid line) under (a) Ar and (b) under O_2 saturation. An aqueous solution of 0.1 M Na_2SO_4 was used as the electrolyte. In both graphs the blue solid line shows the applied potential.

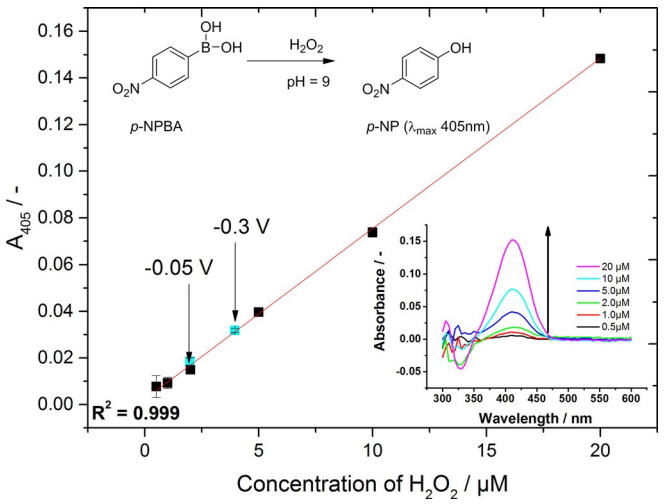

Figure 3. Calibration curve used for quantifying the produced H_2O_2. Reaction leading to *p*-NP formation (upper left inset). Increase in absorbance with increasing concentration of H_2O_2 (lower right inset). Points with turquoise color are the concentrations of H_2O_2 obtained from electrolysis at constant potentials of −0.05 V and −0.3 V vs. NHE.

at −0.05 V and −0.3 V applied bias, respectively. The Figure of merit for comparing different H_2O_2 forming catalysts is a formation rate which is given in $\mu g_{H2O2}\, mg_{cat}^{-1}\, h^{-1}$. Nanostructured TiO_2 supported CuTPP-COOH electrodes reached the formation rates of 2.2 $\mu g_{H2O2}\, mg_{CuTPP\text{-}COOH}^{-1}\, h^{-1}$ and 13.4 $\mu g_{H2O2}\, mg_{CuTPP\text{-}COOH}^{-1}\, h^{-1}$ for the applied potentials of −0.05 V and −0.3 V, respectively. Our system is comparable to well-known semiconductors such as ZnO (21 $\mu g\, mg_{cat}^{-1}\, h^{-1}$)[28] and g-$C_3N_4$ (4.25 $\mu g\, mg_{cat}^{-1}\, h^{-1}$)[19,29] Corresponding control experiments in which the O_2-saturated solution was measured in the dark did not yield any detectable amount of H_2O_2.

To further evaluate the electrochemical characteristics of the O_2 reduction on the TiO_2 NTs/CuTPP-COOH photoelectrodes, we conducted potential-dependent electrochemical impedance spectroscopy (PEIS, Figure 4). Symbols represent experimental data and lines the best fits. The spectra were collected in the potential range between 0.2 and −0.3 V with a step size of 0.1 V. Each potential was kept constant for 10 min to ensure steady state conditions before the impedance measurement, ranging from 100 kHz to 20 mHz, with a peak amplitude of ±10 mV. Measurements were performed under illumination in the Ar- and O_2-saturated electrolyte solution containing 0.1 M Na_2SO_4.

Detailed analysis of Nyquist plots under O_2 saturation reveals the presence of three, not fully developed semi circles (Figure S5, Supporting Information) The first semi-circle (I) at high frequencies between 4.5 kHz and 200 Hz was observable in all spectra and may describe the interfacial TiO_2/CuTPP-COOH charge transfer. A second semi-circle (II) at medium frequencies between 65 Hz and 1.4 Hz is also observable in all spectra and may represent the resistance for electron transport along the TiO_2 NTs and the corresponding surface capacitance.[30] The development of an additional semi-circle (III) at potentials below 0.0 V and lower frequencies between 0.94 Hz and 20 mHz is observable only if the electrolyte is saturated with O_2. This may correspond to the charge transfer resistance of the O_2 reduction reaction. A two-step reaction process is expected to be the reason for the occurrence of semi-circle (III), for example an intermediate state that is involved.[31]

For further quantification of the measured EIS data, corresponding electronic elements were determined by fitting the experimental spectra to the proposed equivalent circuit depicted in Figure 4d. The proposed equivalent circuit is a modified version of the equivalent circuit introduces by Köleli et.al. for CO_2 reduction on polyaniline-coated electrodes.[31]

An additional R/C element at high frequencies has been added to account for the TiO_2/CuTPP-COOH interface at the nanostructured support-electrodes, partly adopted from the transmission line model originally introduced for nanostructured TiO_2 hybrid solar cells.[30] The real capacitors C_{nt} and C_r are modeled with CPEs to account for the non-ideal behavior (i.e. depressed semi-circle) of the capacitive part at medium

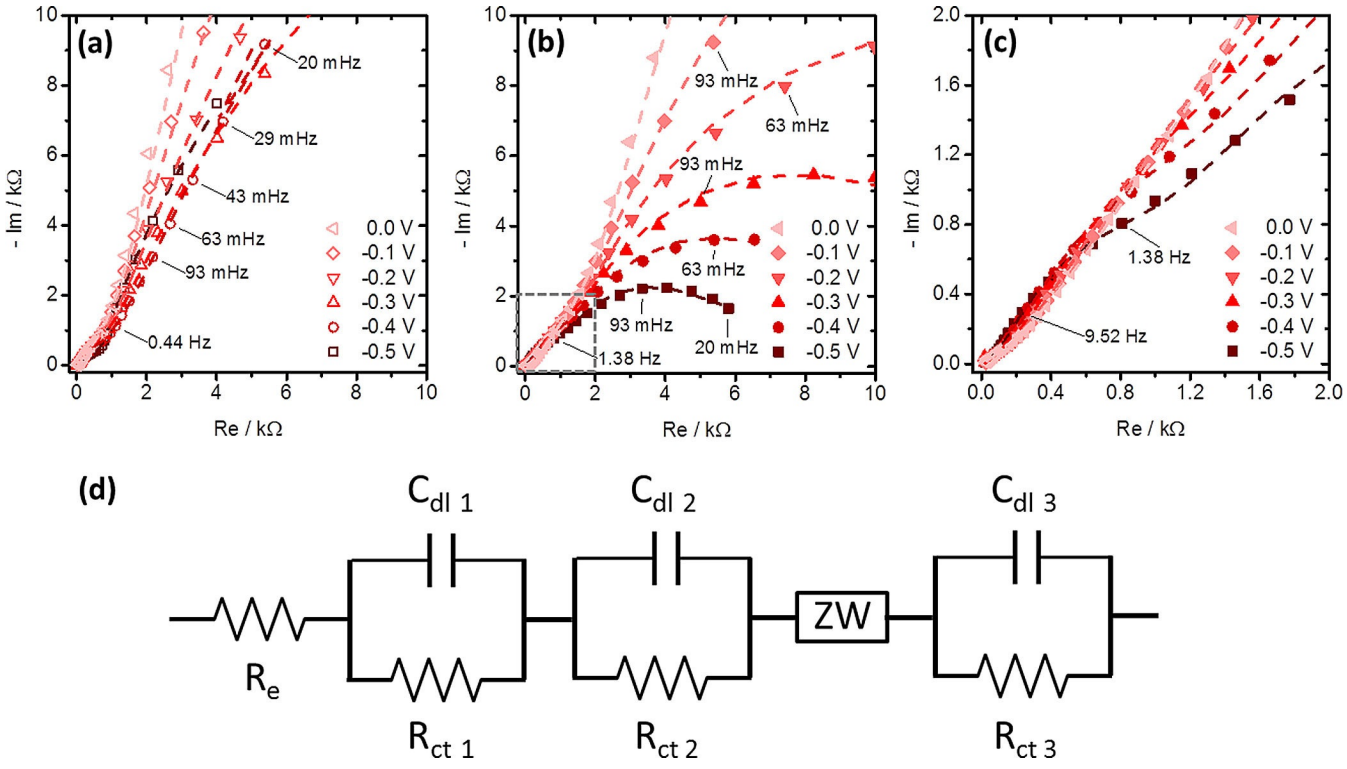

Figure 4. Nyquist plots at different potentials for illuminated, porphyrin covered TiO_2 NTs under (a) Ar and (b) O_2 saturation in the 0.1 M Na_2SO_4 solution. Symbols represent the experimental data and the lines of best fit. (c) Enlarged view of the high frequency domain of (b) indicated therein with a grey, dashed square. (d) Equivalent electric circuit used for fitting the EIS data. R_s: solution resistance, R_f and C_f: interfacial TiO_2/CuTPP-COOH electron charge transfer resistance and the corresponding capacitance, R_{tr} and CPE_{nt}: resistance for electron transport along the TiO_2 NTs and the corresponding capacitance (modelled with a CPE), *ZW*: Warburg element for semi-infinite diffusion, R_r and CPE_r: charge transfer resistance for the O_2 reduction and corresponding capacitance (modelled with a CPE).

and low frequencies.[32] The finite length Warburg impedance (ZW) is used to describe the transport phenomena of O_2 into the porphyrin film and the transport of reduction products out of the film. The parallel configuration of the R_{tr}/CPE_{nt} and R_r/CPE_r elements may be justified owing to the inhomogeneity (porosity) of the CuTPP-COOH covered TiO_2 NTs. From the EIS data we concluded that the ohmic resistance of the electrolyte solution (R_s) is almost constant at all potentials, fluctuating slightly between 17 and 20 Ω. The R_f (interfacial electron charge transfer resistance) is relatively high at positive potentials with 111.6 kΩ at 0.2 V and decreases significantly to 3.1 kΩ at −0.3 V. This suggests enhanced charge transfer over the TiO_2/CuTPP-COOH interface with applied negative bias. R_{tr}, which describes the resistance for electron transport along the TiO_2 NTs, decreases only slightly with the applied potential from initially 2.4 kΩ at 0.2 V to 158 Ω at −0.3 V. This characteristic behavior of R_{tr} is expected for relatively highly doped nanotubes suggesting a small variation of the carrier density with bias (unless full depletion is obtained).[30] The charge transfer resistance related to the O_2 reduction reaction (R_r) could not be determined for positive potentials of 0.2 and 0.1 V, respectively, since the corresponding semi-circle was not developed in the measured frequency limit (20 mHz). Therefore, it was sufficient to fit the electrochemical impedance spectroscopy data at 0.2 V and 0.1 V without the electronic elements used for describing the O_2 diffusion and reduction reaction (ZW, R_r and CPE_r). At 0.0 V the occurrence of semi-circle (III) becomes notable and R_r was determined with 214 kΩ. R_r then decreased significantly to about 2.3 kΩ at −0.3 V, suggesting enhanced O_2 reduction at lower potentials. This is congruent with the observed characteristics from chronoamperometry experiments (Figure 2). Overall, the authors are fully aware that the proposed equivalent circuit may not cope with the complexity of the investigated system and was introduced only as an initial attempt to describe the measured EIS data. Also one has to point out that the EIS measurements were not performed under diffusion controlled conditions (i.e. by a rotating disk electrode), rendering its interpretation challenging. Nonetheless, the proposed equivalent circuit demonstrated good fitting congruency in the Nyquist and Bode plots (Figure 4b and Figure S6, Supporting Information), with, for example, a mean square deviation (X^2/Z) of 0.3% for the EIS data recorded at −0.3 V under O_2 saturation (Figure 4b). A detailed summary of all fitting parameters and their corresponding mean square deviations is given in Table S1, and a comparison of all impedance measurements under Ar and O_2 saturation is shown in Figure S7, in the Supporting Information.

In summary, we have demonstrated a novel photocathode capable of reducing dissolved O_2 to H_2O_2 with evolution rates ranging between 2 and 13 $\mu g_{H2O2}\, mg_{cat}^{-1}\, h^{-1}$. By attaching the CuTPP-COOH catalyst onto TiO_2 NTs through its carboxyl group, we created a heterogeneous molecular catalyst where the formed photocathode is convenient for use in aqueous medium and inherits a significantly higher surface area over planar electrodes owing to self-organized nanostructured TiO_2 NTs. The TiO_2 nanostructures were previously used as catalytic moieties together with sensitizers such as porphyrins and phthalocyanines. However, the use of such molecular porphyrins as photoelectrocatalysts is not common. We have also demonstrated that our system is capable of driving the aforementioned reaction under pH neutral conditions which is expected to reduce the technical complications originating from high acidic or alkaline media.

Experimental Section

Experimental Details such as the synthesis and the details of the electrochemical setup as well as electrochemical impedance spectroscopy can be found in Supporting Information.

Acknowledgements

The authors gratefully acknowledge financial support from the Austrian Science Foundation (FWF) within the Wittgenstein Prize of Prof. Niyazi Serdar Sariciftci (Solare Energie Umwandlung Z222-N19) and the FWF project P29645-N36, Graduate School of Chulalongkorn University (The 90th Anniversary of Chulalongkorn University Fund, Ratchadaphiseksomphot Endowment Fund) and the Thailand Research Fund (RTA6080005).

Conflict of interest

The authors declare no conflict of interest.

Keywords: copper · heterogeneous catalysis · hydrogen peroxide · oxygen reduction · photoelectrochemistry

[1] R. S. Disselkamp, *Energy Fuels* **2008**, *22*, 2771 – 2774.
[2] G. Goor, J. Glenneberg, S. Jacobi, *Ullmann's Encyclopedia of Industrial Chemistry*, Wiley-VCH, Weinheim, Germany, **2012**.
[3] S. Kato, J. Jung, T. Suenobu, S. Fukuzumi, *Energy Environ. Sci.* **2013**, *6*, 3756.
[4] K. Mase, M. Yoneda, Y. Yamada, S. Fukuzumi, *Nat. Commun.* **2016**, *7*, 11470.
[5] K. Mase, M. Yoneda, Y. Yamada, S. Fukuzumi, *ACS Energy Lett.* **2016**, *1*, 913 – 919.
[6] J. R. Kirchner in *Kirk-Othmer Encylopedia of Chemical Technology, Vol. 13, 3rd Ed.* (Eds.: M. Grayson, D. Eckroth), Wiley, New York, **1979**, pp. 12 – 38.
[7] V. R. Choudhary, S. D. Sansare, A. G. Gaikwad, *Catal. Lett.* **2002**, *84*, 81 – 87.
[8] J. H. Lunsford, *J. Catal.* **2003**, *216*, 455 – 460.
[9] S. Chinta, J. H. Lunsford, *J. Catal.* **2004**, *225*, 249 – 255.
[10] P. Landon, P. J. Collier, A. J. Papworth, J. Kiely, G. J. Hutchings, *Chem. Commun.* **2002**, 2058 – 2059.
[11] G. Li, J. Edwards, A. F. Carley, G. J. Hutchings, *Catal. Commun.* **2007**, *8*, 247 – 250.
[12] Y. Yi, L. Wang, G. Li, H. Guo, *Catal. Sci. Technol.* **2016**, *6*, 1593 – 1610.
[13] R. E. Stephens, B. Ke, D. Trivich, *J. Phys. Chem.* **1955**, *59*, 966 – 969.
[14] T. Freund, W. P. Gomes, *Catal. Rev. Sci. Eng.* **1970**, *3*, 1 – 36.
[15] M. Shao, Q. Chang, J.-P. Dodelet, R. Chenitz, *Chem. Rev.* **2016**, *116*, 3594 – 3657.
[16] T. R. Rubin, J. G. Calvert, G. T. Rankin, W. MacNevin, *J. Am. Chem. Soc.* **1953**, *75*, 2850 – 2853.
[17] S. Fukuzumi, *Biochim. Biophys. Acta Bioenerg.* **2016**, *1857*, 604 – 611.
[18] F. Shiraishi, T. Nakasako, Z. Hua, *J. Phys. Chem. A* **2003**, *107*, 11072 – 11081.
[19] Y. Shiraishi, S. Kanazawa, Y. Sugano, D. Tsukamoto, H. Sakamoto, S. Ichikawa, T. Hirai, *ACS Catal.* **2014**, *4*, 774 – 780.

[20] M. Jakešová, D. H. Apaydin, M. Sytnyk, K. Oppelt, W. Heiss, N. S. Sariciftci, E. D. Glowacki, *Adv. Funct. Mater.* **2016**, *26*, 5248 – 5254.
[21] M. K. Węcławski, M. Jakešová, M. Charyton, N. Demitri, B. Koszarna, K. Oppelt, S. Sariciftci, D. T. Gryko, E. D. Głowacki, *J. Mater. Chem. A* **2017**, https://doi.org/10.1039/C7TA05882A.
[22] C. Song, L. Zhang, J. Zhang, D. P. Wilkinson, R. Baker, *Fuel Cells* **2007**, *7*, 9 – 15.
[23] Q. Qu, H. Geng, R. Peng, Q. Cui, X. Gu, F. Li, M. Wang, *Langmuir* **2010**, *26*, 9539 – 9546.
[24] A. Auer, N. S. W. Jonasson, D. H. Apaydin, A. I. Mardare, G. Neri, J. Lichtinger, R. Gernhäuser, J. Kunze-Liebhäuser, E. Portenkirchner, *Energy Technol.* **2017**, *5*, 2253 – 2264.
[25] P. M. Wood, *Biochem. J.* **1988**, *253*, 287 – 289.
[26] H. G. Kuivila, *J. Am. Chem. Soc.* **1954**, *76*, 870 – 874.
[27] H. G. Kuivila, A. G. Armour, *J. Am. Chem. Soc.* **1957**, *79*, 5659 – 5662.
[28] A. J. Hoffman, E. R. Carraway, M. R. Hoffmann, *Environ. Sci. Technol.* **1994**, *28*, 776 – 785.
[29] Y. Shiraishi, S. Kanazawa, Y. Kofuji, H. Sakamoto, S. Ichikawa, S. Tanaka, T. Hirai, *Angew. Chem. Int. Ed.* **2014**, *53*, 13454 – 13459; *Angew. Chem.* **2014**, *126*, 13672 – 13677.
[30] F. Fabregat-Santiago, G. Garcia-Belmonte, I. Mora-Seró, J. Bisquert, *Phys. Chem. Chem. Phys.* **2011**, *13*, 9083.
[31] F. Köleli, T. Röpke, C. H. Hamann, *Electrochim. Acta* **2003**, *48*, 1595 – 1601.
[32] F. B. Growcock, R. J. Jasinski, *J. Electrochem. Soc.* **1989**, *136*, 2310.

Manuscript received: December 28, 2017
Accepted manuscript online: December 29, 2017
Version of record online: February 20, 2018

